

On chip porous polymer membranes for integration of gastrointestinal tract epithelium with microfluidic ‘body-on-a-chip’ devices

Mandy Brigitte Esch · Jong Hwan Sung · Jennifer Yang · Changhao Yu · Jiajie Yu · John C. March · Michael Louis Shuler

Published online: 31 July 2012
© Springer Science+Business Media, LLC 2012

Abstract We describe a novel fabrication method that creates microporous, polymeric membranes that are either flat or contain controllable 3-dimensional shapes that, when populated with Caco-2 cells, mimic key aspects of the intestinal epithelium such as intestinal villi and tight junctions. The developed membranes can be integrated with microfluidic, multi-organ cell culture systems, providing access to both sides, apical and basolateral, of the 3D epithelial cell culture. Partial exposure of photoresist (SU-8) spun on silicon substrates creates flat membranes with micrometer-sized pores (0.5–4.0 μm) that—supported by posts—span across 50 μm deep microfluidic chambers that are 8 mm wide and 10 long. To create three-dimensional shapes the membranes were air dried over silicon pillars with aspect ratios of up to 4:1. Space that provides access to the underside of the shaped membranes can be created by isotropically etching the sacrificial silicon pillars with xenon difluoride. Depending on the size of the supporting posts and the pore sizes the overall porosity of the membranes ranged from 4.4 % to 25.3 %. The microfabricated membranes can be used for integrating barrier tissues such as the gastrointestinal

tract epithelium, the lung epithelium, or other barrier tissues with multi-organ “body-on-a-chip” devices.

Keywords Membrane · 3-D tissue culture · Gastrointestinal tract · Barrier tissue · Micro cell culture analog · μCCA · Body-on-a-chip

1 Introduction

Microfluidic cell culture systems that contain compartments for the culture of multiple tissues such as the gastrointestinal tract epithelium, liver, kidney and tumor tissues are currently being developed for the purpose of studying the collective response of multiple organs to new drugs under near physiologic conditions (Ma et al. 2009; Sin et al. 2004; Tatosian and Shuler 2009; Vozzi et al. 2009; Zhang et al. 2009). Low bioavailability of drugs at the target organ has been cited as one of the major reasons for the failure of newly developed drugs in clinical trials (Kola and Landis 2004). Drug testing systems that contain models of barrier tissues such as the gastrointestinal tract epithelium and the lung epithelium are invaluable for correctly predicting the bioavailability of newly developed drugs early in the drug development process.

Microfluidic tissue analogs of barrier tissues replicate the physiologic aspects of these tissues with more authenticity than static models that are currently being used. In microfluidic systems the ratios of *in vivo* masses or volumes of organs can be recreated on chip, and physiologic fluid residence times in each organ can be achieved. Moreover, metabolites produced in one tissue can travel to other organ compartments and affect the tissues cultured there. Such devices have the potential to improve the drug screening

Mandy Brigitte Esch and Jong Hwan Sung have contributed equally to the work.

M. B. Esch (✉) · J. Yang · C. Yu · M. L. Shuler
Department of Biomedical Engineering, Cornell University,
Ithaca, NY 14853, USA
e-mail: mbe2@cornell.edu

J. H. Sung
Department of Chemical Engineering, Hongik University, Seoul,
South Korea

J. Yu · J. C. March
Department of Biological and Environmental Engineering,
Cornell University, Ithaca, NY 14853, USA

process significantly, because they recreate parts of the human metabolism.

A few microfluidic *in vitro* analogs of barrier tissues have been developed so far, (Huh et al. 2010; Imura et al. 2009; Ramello et al. 2011). But none of these models were combined with other tissue models within one fluidic system. The developed devices typically contain semipermeable membranes that were sandwiched between two microfluidic chambers. The membranes provide a surface for cell growth and at the same time they separate the chambers that contain differing concentrations of compounds that are used in the study. The pores in the membranes allow for the transport of molecules across the cell layer. Using semipermeable membranes, the development of *in vitro* cell culture analogs of tissues of the lung, the gastrointestinal tract and the kidney has been achieved (Ferrell et al. 2010; Huh et al. 2010; Imura et al. 2009; Ramello et al. 2011). However, sandwiching membranes between two existing tissue chambers can be challenging. It is not always possible to assemble such systems so that they are leak-free.

Because sheets of membranes are difficult to integrate with microfluidic systems, multi-organ cell culture devices are limited in regards to the barrier tissues they contain. As a consequence the microfluidic systems that connect the basolateral chamber of a barrier tissue model with another tissue chamber utilize off chip modules that are connected to on-chip components. For example, Mahler et al. and Brand et al. have developed off-chip chambers that utilize transwell membrane inserts for the culture of intestinal epithelial cells under fluidic conditions (Brand et al. 2000; Mahler et al. 2009a). Both systems have been used in combination with liver cell chambers to create *in vitro* models of intestinal absorption and first pass metabolism of drugs. Both systems cannot scale the surface area of the intestinal epithelium to approximate the *in vivo* ratio of epithelial surface area to the mass and volume of liver tissue because the sizes of transwell membranes that are used within the modules are fixed. Membranes that are fabricated directly on top of microfluidic chambers could be scaled appropriately and would not be prone to leaking.

Porous silicon nitride membranes address one of these issues because they can span microfluidic compartments of varying sizes and have been used for the culture of endothelial cells in an effort to recreate part of the blood brain barrier *in vitro* (Harris and Shuler 2003). However, silicon nitride membranes are typically patterned at the front side of silicon wafers and released by etching from the backside. Integrating these membranes with microfluidic systems requires one or two bonding steps to create closed fluidic chambers. This process is not straightforward if the desired chamber depth is less than the thickness of the silicon substrate ($\sim 500\ \mu\text{m}$), which is typically the case in “body-on-a-chip” devices. Flexibility in choosing chamber dimensions such as the chamber depth is necessary to be able to adjust fluid residence times within individual organ compartments.

Typical values for chamber depths range from 20–200 μm (Sin et al. 2004).

In addition, both commercially available membranes and microfabricated membranes are typically flat and do not recreate the three-dimensional aspects of tissues such as the macro villi of the gastrointestinal tract epithelium. The gastrointestinal tract epithelium contains both micro and macro villi that increase the absorptive area of the intestine (Wang et al. 2010). Conventional models of the gastrointestinal tract such as Caco-2 monolayers do not provide three-dimensional surfaces that take the geometric character of the tissue into account. To recreate the three-dimensionality of the intestinal epithelium more authentically *in vitro*, we have previously developed a novel fabrication method to create a hydrogel scaffold that mimic intestinal villi (Sung et al. 2011). The soft mechanical property of the hydrogel made it difficult to control the exact 3-dimensional shape and the system is difficult to integrate into a microfluidic chip. Systems in which cells are either cultured as a flat monolayer covering a membrane, or embedded inside a matrix of hydrogels that covers a membrane are easy and simple to create, but do not accurately represent the intestinal tissue *in vivo*. Mimicking the tissue organization of the intestinal epithelium authentically requires microscale three-dimensional semipermeable membranes that act as cell culture surface and control mass transport.

Here, we report a novel method for the fabrication of porous membranes that can be flat or contain 3-D villi with aspect ratios of up to 4:1. They can be integrated with on-chip multi-organ tissue culture devices that require the presence of the intestinal barrier tissue in addition to other tissues, such as models of the first pass metabolism. The novelty of the fabrication method lies in the use of one SU-8 layer for the fabrication of a microfluidic chamber and a porous membrane that spans across the chamber. We use complete cross-linking to form the chamber and a subsequent partial cross-linking of the SU-8 top layer to form the membrane. Subsequent removal of SU-8 that was not cross-linked and drying yields a flat, porous membrane. When the chamber and membrane are fabricated on a substrate that contains silicon topography, the membrane can be collapsed onto that topography so that it takes on its three-dimensional structure (Fig. 1(a and b)). Using this method, it was possible to fabricate flat and three-dimensionally structured porous membranes, which—supported by posts underneath—span 50 μm deep microfluidic chambers that were 8 mm wide and 10 mm long. Pore sizes were uniformly distributed and ranged in size from $0.5 \times 0.5\ \mu\text{m}$ to $3 \times 3\ \mu\text{m}$. It was possible to control the 3-D shape of the membranes by fabricating pillars of different sizes on the silicon substrate using deep reactive ion etching or KOH etching and letting the membrane drape over them during drying on air or with nitrogen (Fig. 1(b)). We also showed that the sacrificial silicon pillars can be removed via xenon difluoride etching.

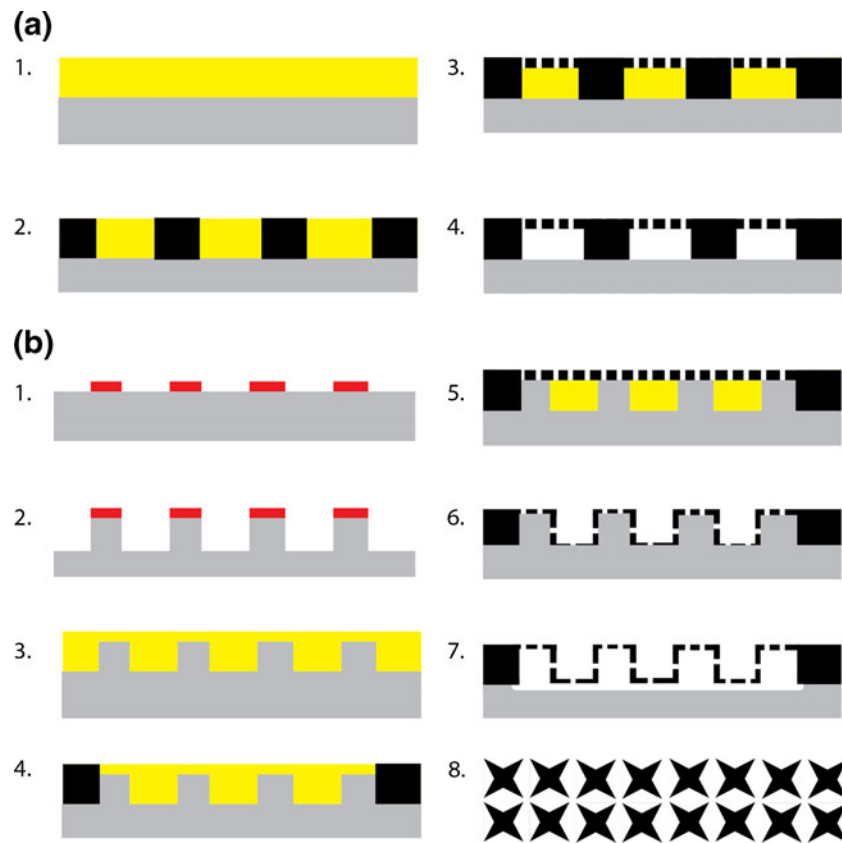


Fig. 1 Two-exposure step fabrication of microfluidic chambers and membranes using a single layer of SU-8. **(a)** Microfluidic chambers covered by flat, porous membranes for 2-D models of the gastrointestinal tract epithelium. **(b)** Microfluidic chambers covered by 3-D shaped, porous membranes for models of the gastrointestinal tract epithelium that recreate key aspects of the villi structure. Step by step description: **(a)** 1) SU-8 spinning (2800 rpm for 60 s) and slowly ramped soft bake at 95 °C for 5 min; 2) exposure of chamber walls and support posts; 3) exposure of membrane with pores with an exposure time that cross-links the top layer only; 4) removal of sacrificial SU-8 with developer; **(b)** 3-D membranes: 1) Patterning of

photoresist (red) on silicon; 2) deep reactive ion etching of pillars; 3) Omnicoat spinning and SU-8 spinning followed by a slowly ramped soft bake; 4) exposure of microfluidic chamber walls; 5) exposure of membrane layer with pores; 6) removal of sacrificial SU-8 with developer and subsequent drying with nitrogen; 7) removal of omnicoat to detach the membrane from silicon pillars or removal of silicon pillars with xenon difluoride. 8) Pore shapes that were used in the fabrication of three-dimensionally shaped membranes to ameliorate irregular pore formation due to the diffraction of light. (Silicon = grey, unexposed SU-8 = yellow, cross-linked SU-8 = black)

The silicon etching created fluidic access underneath the membranes which retained their three-dimensional character even after wetting with water.

We cultured Caco-2 cells on both flat and three-dimensionally shaped membranes (without removal of the underlying silicon structure) and characterized their growth and the expression of occludin, a protein that indicates that tight junctions have been established between cells (Furuse et al. 1993). Because drug absorption can be predicted with Caco-2 cell monolayers, (Conradi et al. 1993; Kim et al. 1993; Rubas et al. 1996; Wils et al. 1994) the cell line has been widely used for *in vitro* drug absorption assays (Artursson et al. 2001). Under appropriate conditions, Caco-2 cells form tight junctions and micro villi similar to the enterocytes lining the normal gastrointestinal (GI) tract epithelium (Hubatsch et al. 2007). As a way to improve the current *in vitro* model, we developed a Caco-2 cell model that mimics the 3-D geometry

of intestinal villi. Our results show that cells were viable and formed a 3-D cellular structure conforming to the underlying geometry of the SU-8 membrane. After 21 days of culture, 100 % of the membrane surface was covered with Caco-2 cells, which expressed occludin, indicating the formation of tight junctions. The developed 2-D and 3-D models can be integrated with microfluidic devices that contain tissue compartments for multiple organs.

2 Material and methods

2.1 Fabrication of microfluidic chambers with flat porous membranes

The fabrication technique consists of a two-step exposure of a 50 μm thick SU-8 layer spun on a silicon wafer. The first

exposure defines the walls of the microfluidic chamber as well as membrane support posts inside the chamber. The second exposure is a partial exposure that cross-links the top 0.5–4 μm of the remaining SU-8. In detail, a 50 μm thick layer of SU-8 2050 (Microchem, Newton, MA) was spun-coated onto a silicon wafer at 2800 rpm for 60 sec and soft baked at 65 $^{\circ}\text{C}$ for 2 min, then 95 $^{\circ}\text{C}$ for 5 min before patterning using the EV620. Patterning of the SU-8 via the contact aligner was separated into two exposure steps: a long exposure (720 mJ/cm^2) that defined the microfluidic chamber and supporting SU-8 posts, and a short exposure (15.6 mJ/cm^2) that defined a thinner layer (\sim up to 3 μm) of SU-8 with pores (Fig. 1(a)). After exposing both layers, the wafer was baked (65 $^{\circ}\text{C}$ for 1 min, then 95 $^{\circ}\text{C}$ for 7 min) and developed in SU-8 developer (Microchem) for at least two hours. The wafer was then rinsed with isopropyl alcohol (IPA) and dried using a critical point dryer.

2.2 Fabrication of microfluidic chambers with porous membranes for three-dimensional Caco-2 cell culture

Porous membranes were formed over silicon pillars with square cross sections of different sizes (25, 50, or 100 μm wide) and densities (25, 50, 100, or 200 μm between pillars) using conventional photolithography techniques (Fig. 1(b)). Briefly, silicon wafers were primed with P-20 primer (Shin EtsuMicroSi, Tokyo, Japan) at 3000 rpm for 30 sec and then spin coated with a 2- μm -thick layer of SC 1827 photoresist (3000 rpm for 30 sec)(Shipley, Marlborough, MA) baked for 1 min at 115 $^{\circ}\text{C}$. Pillar arrays were then patterned into the photoresist at 96 mJ/cm^2 with an EV620 contact aligner (Electronic Visions Inc., Phoenix, AZ) and developed in AZ 300 MIF (AZ Electronic Materials, Somerville, NJ) for 1–2 min. Pillars 100 μm tall were etched into the silicon via a Bosch fluorine etch (Unaxis 770 Si Etcher, Plasma-Therm Inc., St. Petersburg, FL) and the remaining SC 1827 was stripped via an oxygen plasma (GaSonic Aura 1000 Asher).

After dehydrating the wafer at 170 $^{\circ}\text{C}$ for 15–20 min to improve adhesion, a sacrificial layer (Omnicoat) was spun onto the wafer. Then a 110- μm -thick layer of SU-8 2050 (Microchem, Newton, MA) was spun onto the wafer at 1700 rpm for 60 sec and soft baked at 65 $^{\circ}\text{C}$ for 5 min, then 95 $^{\circ}\text{C}$ for 20 min before patterning using the EV620. Patterning of the SU-8 via the contact aligner was conducted with two exposure steps: a long exposure (720 mJ/cm^2) that defined the microfluidic chamber around the pillar array, and a short exposure (15.6 mJ/cm^2) that cross-linked the top layer (0.5–2.5 μm) of SU-8 with the exception of pores. After conducting both exposures immediately following each, the wafer was baked (65 $^{\circ}\text{C}$ for 5 min, then 95 $^{\circ}\text{C}$ for 10 min) and developed in SU-8 developer (Microchem) for at least two hours, then rinsed with isopropyl alcohol (IPA). The wafers were then left to dry on air under a lamp for at least 30 min. The omnicoat (Microchem, Newton,

MA) release layer was removed with developer so that the membrane was detached from the silicon pillars, creating space for fluidic flow. Images of membranes were obtained with an optical microscope (Fisher Scientific, Hampton, NH) and microscope camera (Nikon); cross sections were obtained by cleaving and imaging with a Zeiss Ultra 55 scanning electron microscope (Carl Zeiss, Thornwood, NY).

2.3 Fabrication of microfluidic chambers with three-dimensional porous membranes and increased chamber depth

Silicon pillars were created with an alternative method to the one described above. Using this method a silicon nitride film was grown (500 nm) at 1100 $^{\circ}\text{C}$ on silicon <100> wafers (Silicon Quest, Santa Clara, CA) using the process gases SiH_2Cl_2 , NH_3 , and N_2O in a furnace tube. The wafers were then coated with photoresist S1813 (Shipley, Marlborough, MA) at a spin speed of 3000 rpm and the area surrounding the pillars was exposed for 4 s using an AB-M HTG 3HR contact aligner (AB-M, San Jose, CA). They were then developed for 2 min and the exposed silicon nitride was removed using a reactive ion etcher (Oxford 80, Oxford Instruments, Tubney Woods, Abingdon, Oxfordshire, OX13 5QX, UK) with 50 sccm CHF_3 and 2 sccm O_2 at 50 mTorr and 200 W. The exposed substrate was etched to a depth of 20 μm using a 50 % KOH solution at 80 $^{\circ}\text{C}$. The remaining silicon nitride was removed with a reactive ion etcher (Oxford 80, Oxford Instruments, Tubney Woods, Abingdon, Oxfordshire, OX13 5QX, UK) with 50 sccm CHF_3 and 2 sccm O_2 at 50 mTorr and 200 W. SU-8 was then spun and exposed as described above. After air-drying the SU-8 membrane, the wafer was exposed to xenon-difluoride using a Xactix xenon difluoride etcher (XACTIX, Inc., Pittsburgh, PA 15203 USA). We used 40 cycles with 20 s per cycle at 4 Torr xenon difluoride gas pressure. The samples were then cleaved to expose their cross-section, which was imaged with a Zeiss Ultra 55 scanning electron microscope (Carl Zeiss, Thornwood, NY).

2.4 Cell culture and chemicals

Caco-2 cells (ATCC HTB 37, Manassas, VA) were thawed at passage 28 and used for experiments at passage 41–60. Cells were maintained in Dulbecco's modified Eagle medium with 4 mM GlutaMAX and 4.5 g/L D-glucose (DMEM, Invitrogen, Grand Island, NY) supplemented with 20 % heat inactivated fetal bovine serum (HI FBS, Invitrogen) every 2–3 days. Rabbit anti-occludin monoclonal antibody, secondary antibodies (Alexa 555- or Alexa 568-conjugated goat anti-rabbit IgG), and normal goat serum were obtained from Invitrogen. The blocking solution for immunostaining wash steps, 1 % DPBSA, was made from 1 % (w/v) bovine serum albumin (BSA)(Sigma Aldrich, St. Louis, MO) dissolved in DPBS (Invitrogen).

2.5 Caco-2 cell culture on membranes and characterization of the cell layer

Membrane samples were sterilized by soaking them in IPA for at least 15 min. They were then washed three times with PBS and coated with $4 \mu\text{g}/\text{cm}^2$ of poly-D-lysine (Sigma Aldrich) for 5 min, washed with an equal volume of DPBS, coated with $8 \mu\text{g}/\text{cm}^2$ of Type I collagen (BD Biosciences, Bedford, MA) for 1 h and washed again with DPBS to promote cell attachment and migration. Caco-2 cells were then seeded on samples at a density of $281,000 \text{ cells}/\text{cm}^2$, which covered the base of the villi after 24 h. Cell proliferation was monitored by staining the cells with CellTracker (Molecular Probes) 24 h after seeding. Each sample was re-stained every 4–5 days thereafter. After 8, 15, 18, and 22 days of cell culture (separate samples), the samples were fixed in formaldehyde, washed 3 times for 5 min in 1 % DPBSA, and then permeabilized with Triton X-100 in 2.5 % DPBSA for 5 min. The samples were washed 3 times again, incubated with rabbit anti-occludin antibody (or 5 % normal goat serum in blocking solution for negative control) for 45–55 min, and incubated with goat anti-rabbit antibody tagged with either Alexa Fluor 555 (only samples that were stained on day 8) or Alexa Fluor 568 for 45–55 min with 3 times 5 min washes after each step. After occludin staining, the samples were incubated simultaneously with Alexa Fluor 488 phalloidin (Invitrogen) and TO-PRO-3 (Invitrogen) to stain for filamentous actin (F-actin) and nuclear DNA, respectively. Samples were then scanned with a Leica SP2 confocal microscope (Leica Microsystems, Bannockburn, IL) and 3-D images were rendered using Volocity (Perkinelmer, Waltham, MA).

2.6 Simulation of flow in microfluidic chambers with three-dimensionally structured membranes

The fluid velocity and diffusion profiles inside a microfluidic device integrated with SU-8 membranes were simulated using Comsol multiphysics (Burlington, MA, USA). The geometries of the flat and 3-D SU-8 membranes were drawn in 2-D, and the incompressible Navier-Stokes and convection-diffusion multiphysics were used. The parameters used in the simulation are summarized in Table 1.

Table 1 Simulation parameters

Parameters	Value	Unit
Density	1000	kg/m^3
Viscosity	1×10^{-3}	Pa s
Inflow velocity	7.5×10^{-5}	m/s
Diffusion coefficient	3×10^{-10}	m^2/s
Incoming fluid concentration in top chamber	1	mM

3 Results and discussion

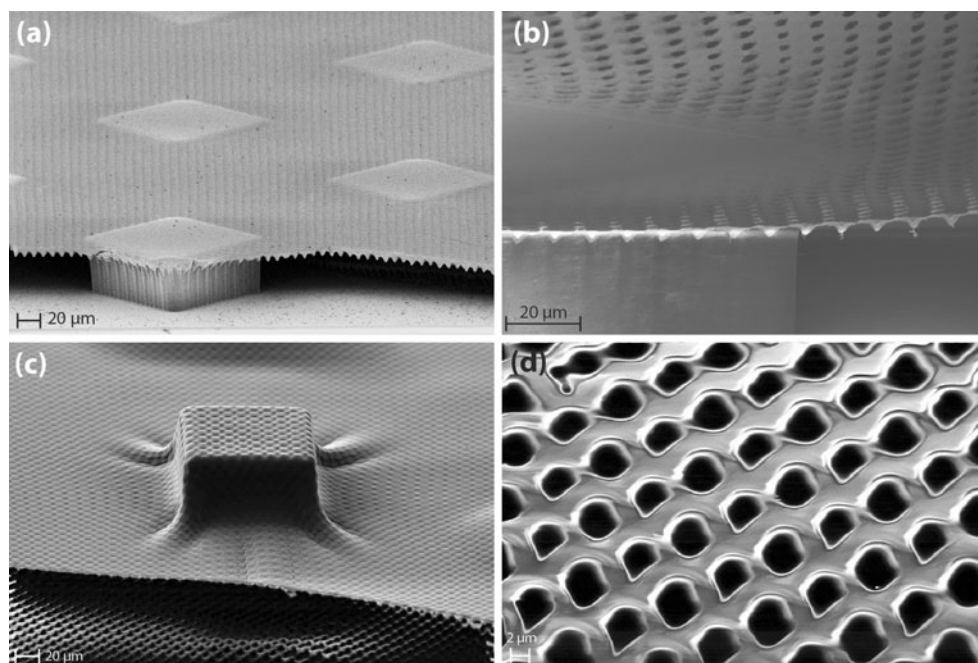
3.1 Fabrication of microfluidic chambers that contain flat, porous membranes

Using the method presented here we fabricated microfluidic chambers (8 mm wide, 10 mm long, $50 \mu\text{m}$ deep) that were covered by flat SU-8 membranes. The membranes were $0.5\text{--}2.5 \mu\text{m}$ thick with pore sizes that ranged from $0.5\text{--}4 \mu\text{m}$. Both, microfluidic chambers and porous membranes were fabricated in one fabrication sequence that can be completed in one day. The principle fabrication protocol relies on a two-step exposure. The first exposure cross-links the walls of the microfluidic chamber as well as the structural support posts for the membrane (for this set of experiments, the supporting posts were $50 \times 50 \mu\text{m}$ wide and $75 \mu\text{m}$ apart from each other). The second exposure cross-links the top layer of the resist that was not exposed during the first exposure step. This is achieved by using a very short exposure time (typically between 10 s to $20 \text{ mJ}/\text{cm}^2$, 365 nm light) that is not sufficient to cross-link the entire SU-8 layer. Cross-linking the top layer creates a thin SU-8 membrane that is attached to the microfluidic chamber walls that were cross-linked in the first exposure step (see Fig. 1). Using a photolithography mask that contains pores for the short exposure step creates pores within the membrane. The pores allow for the subsequent removal of the unexposed SU-8 underneath the membrane. Partial SU-8 exposure has been previously used to fabricate microelectromechanical systems (MEMS) (Carlier et al. 2004; Kim et al. 2004) and structures that have been used as molds for complex microfluidic PDMS devices (Anderson et al. 2000; Bohl et al. 2005). Utilizing the high contrast capability of SU-8 and partial exposure of the material, we created microfluidic chambers that are covered by porous membranes.

The thickness of the fabricated membranes ranged from $0.5 \mu\text{m}$ at their thinnest region to $2.5 \mu\text{m}$ and is well suited to enable mass transport with low resistance. The membranes are thicker than those that can be fabricated with silicon nitride ($200 \text{ nm}\text{--}1 \mu\text{m}$), (Harris and Shuler 2003; Zhang et al. 2008) but thinner than commercially available membranes. The energy used to cross-link the membrane determines its thickness because it decays with distance from the top and reaches a level that becomes insufficient to cross-link material that is farther away from the light source. Exposure energies used to create membranes ranged from 10 s to $20 \text{ mJ}/\text{cm}^2$. Membranes that were underexposed and overexposed were subject to cracking during drying. Membranes that were at least $0.5 \mu\text{m}$ thick at their thinnest areas were robust enough to withstand the process of drying without cracking (Fig. 2(a)).

The described fabrication process creates membranes with pore sizes ranging from $0.5\text{--}4 \mu\text{m}$. Since SU-8 layers

Fig. 2 Porous SU-8 membranes that are anchored to and span across microfluidic chambers. The membranes are either flat (**a** and **b**), or they were dried over sacrificial silicon pillars and take on the shape of the pillars (**c** and **d**). (**b**) A higher magnification scanning electron microscopy image of a flat membrane with 3 μm pores. (**d**) Close-up of the 3D shaped membrane imaged in (**c**) The image reveals the membrane's porous character. The sacrificial silicon pillars can be removed via xenon difluoride etching



are not perfectly flat and diffraction of light occurs during contact photolithography, the exposure energy used to cross-link the membranes also influences the pore size. However, since the range of exposure energies that cross-link the SU-8 that later constitutes the membrane is small, the pore size is not affected beyond control and can be adjusted by increasing or decreasing the pore size in the array of pores in the mask. For example, masks that contained an array of $3 \times 3 \mu\text{m}$ pores were exposed with $20 \text{ mJ}/\text{cm}^2$ resulted in rounded pores that were $2.5 \mu\text{m}$ in diameter. The magnitude of decrease in size depends on each sample since the flatness (or lack of flatness) of a sample contributes to the decrease. To create membranes with a desired thickness and pore size, we suggest that the energy that is necessary to result in a particular thickness of the membrane be determined first and then to adjust the pore size by adjusting the sizes of pores on the mask. Despite the rounding of the pores and variability in sample flatness, the pore sizes we achieved were relatively uniform throughout the membrane (Fig. 2(b)).

In our design the support posts that serve as structural support were $50 \times 50 \mu\text{m}$ in size. They were spaced $75 \mu\text{m}$ apart from one another. In the places at which they support the membrane, the membrane is not porous. Hence in our example the support posts decreased the area of the membrane that contains pores by 32 %. The porosity of the porous area alone depends on the pore size and was estimated to be between 9.7 %–56.7 %. The porosity of the entire membrane area, including the post area was between 4.4 %–25.3 %. The maximum porosity we achieved is about half of that achieved with silicon nitride membranes that have been used for the support of barrier tissues, (Harris and Shuler 2003) but higher than that of commercially available

membranes (~ 10 % porosity at a membrane thickness of $10 \mu\text{m}$). It is possible to increase the porosity of the presented membranes by decreasing the percentage of the area without pores by decreasing the size of the support posts and spacing them farther apart. When spacing them farther apart it may be necessary to dry the devices via critical point drying, so that the membranes do not collapse onto the substrate during air-drying. Higher porosity is desired to place the primary resistance for mass transfer on the cell layer rather than the membrane.

3.2 Fabrication of microfluidic chambers with membranes that are shaped in the form of small villi structures

Drying the membranes over support posts that are spaced at least $150 \mu\text{m}$ from one another produces membranes that drape over the posts, forming curved membrane surfaces hanging over the posts (Fig. 2(b)). The curvature and the height of the membranes are determined by the height, size and the distance between of the posts. When the posts consist of silicon instead of SU-8, i.e. if the SU-8 membrane fabrication is preceded by a step that creates silicon pillars via deep reactive ion etching or KOH etching (Fig. 1(b)), a small space can be created between the membrane and the silicon. For this purpose a sacrificial layer (Omnicoat) was spun onto the silicon before SU-8 spinning. This layer can be removed after the membranes have formed. The membrane is separated from the underlying surface and can allow small amounts of liquid to access the underside of the membrane.

The width of the pillars we tested was 25, 50, and $100 \mu\text{m}$. The distance between the pillars was 25, 50, 100, and $200 \mu\text{m}$. The height of the pillars was between 40 and $100 \mu\text{m}$. The

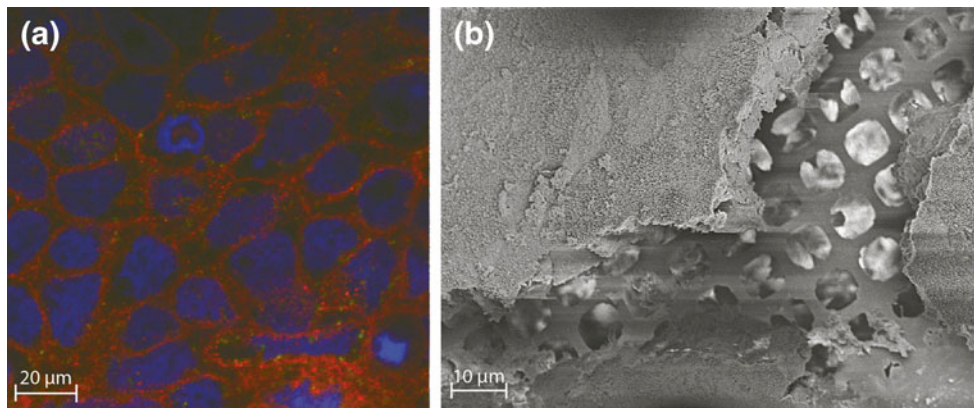


Fig. 3 Comparable to Caco-2 cell growth on commercially available membranes, Caco-2 cells grown for 21 days on flat, porous SU-8 membranes that spanned across microfluidic chambers (8 mm wide and 10 mm long) covered 100 % of the membrane’s surface without mechanically stressing it. The cells expressed a tight junction protein (occludin) throughout the cell layer, indicating that the barrier function

that is needed for drug absorption studies was established. **(a)** Fluorescence microscopy image of Caco-2 cells that were immunostained for occludin (red). The nuclei of the cells were stained blue. **(b)** Scanning electron microscopy image of Caco-2 cells and the underlying membrane. The cells were damaged during the fixation process, revealing the intact, porous membrane underneath

fabricated pillar structures had aspect ratios ranging from 1: 0.5 to 1:4. The spacing between the pillars needed to be at least twice the width of the pillars to ensure that the SU-8 membranes reached the substrate between the pillars. Our

ultimate goal was to re-create *in vivo* sizes of gastrointestinal villi, which are 500 μm high (Tortora and Grabowski 1993). Increasing the height of the pillar structures was challenging, as higher pillars required a larger surface area of SU-8 to hang

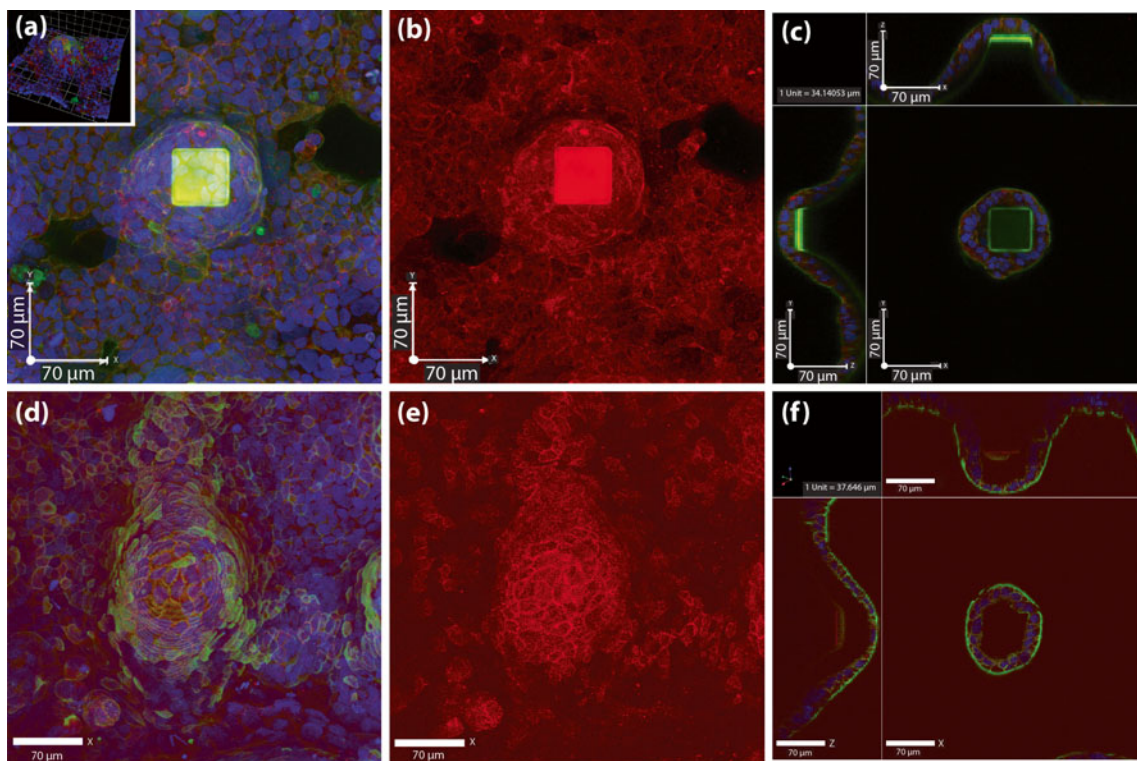
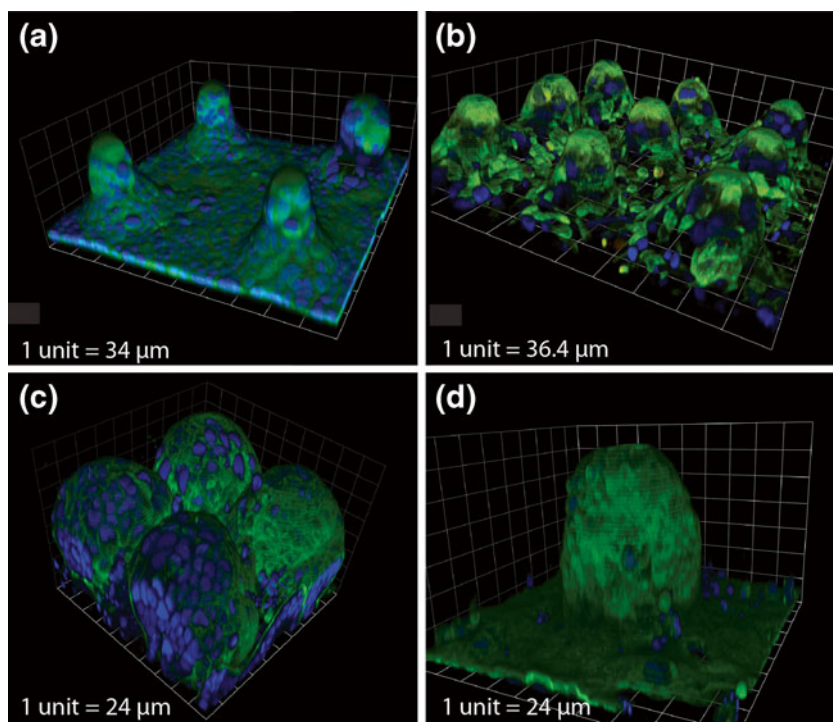


Fig. 4 Three-dimensional cell culture of gastrointestinal epithelial cells (Caco-2) that were grown for 8 days **(a, b, c)** and 21 days **(d, e, f)** on porous SU-8 membranes that were dried on silicon pillars (50 μm wide and 200 μm high). Occludin, a tight junction protein is shown in red, actin is shown in green, and nuclei are shown in blue. **(a and b)** Composite extended view of confocal microscopy images of 8 day old Caco-2 cultures show that at the time of staining coverage is incomplete and tight

junctions are not fully established yet (inset in A: overhead view of 8-day-old Caco-2 showing occludin staining on the villus tip). **(d and e)** show that after 21 days of culture, coverage is complete and cells have developed tight junctions throughout the cell layer. The presence of tight junctions indicates that the cell layer’s barrier function that is necessary for physiologically correct drug absorption studies has been established. Images **(c)** and **(d)** show cross-sections

Fig. 5 Composite images of Caco-2 cell cultures on 3-D SU-8 membranes draped over silicon pillars. The images show that Caco-2 cells grow on 3-D SU-8 membranes that were dried over silicon pillars of different sizes and with different spacing. **(a)** $25 \times 25 \times 80 \mu\text{m}$ pillars with $200 \mu\text{m}$ distance **(b)** $50 \times 50 \times 80 \mu\text{m}$ pillars with $100 \mu\text{m}$ distance **(c)** $100 \times 100 \times 100 \mu\text{m}$ pillars with $100 \mu\text{m}$ distance **(d)** $100 \times 100 \times 100 \mu\text{m}$ pillar with $200 \mu\text{m}$ distance. Actin is shown in green and nuclei are shown in blue



over the pillars and the material was more prone to tearing during drying. It is also necessary to create SU-8 membranes that are thinner to render it more flexible. Thinner SU-8 membranes were used for the highest aspect ratio pillars we worked with. They were obtained by decreasing the exposure energy from 20 mJ/cm^2 to 15.6 mJ/cm^2 .

Since SU-8 spinning over high aspect ratio silicon pillars creates relatively uneven SU-8 layers compared to SU-8 that was spun on a flat surface, the pore sizes of the pores that are created during the exposure with a contact photolithography tool were not as uniformly distributed as on the flat membranes described above. To decrease the effect of light diffraction on the pore geometry, we adjusted the pore geometry on the lithography mask. The diagram in Fig. 1(b/8) shows a suitable pore geometry for the mask. This geometry prevents additive cross-linking in the spaces between pores.

3.3 Two-dimensional and three-dimensional Caco-2 cell models of the intestinal epithelium

To create two dimensional and three-dimensional microfluidic models of the intestinal epithelium, we modified the surfaces of the fabricated membranes with poly-D-lysine and collagen and seeded Caco-2 cells on them. Caco-2 cells are cells from a colon carcinoma cell line that has been used extensively for drug and nutrient absorption studies (Artursson et al. 2001; Mahler et al. 2009b).

On both, flat membranes and three-dimensional membranes, Caco-2 cells grew with normal morphology and reached 100 % coverage within 21 days of seeding. This

observation is comparable to Caco-2 cell growth observed on commercially available membranes that were modified with collagen prior to cell seeding. The membranes were mechanically strong enough to support cell growth without breaking (Fig. 3(b)). Figure 3(a) shows Caco-2 cells that were immunostained for actin (green) and occludin (red).

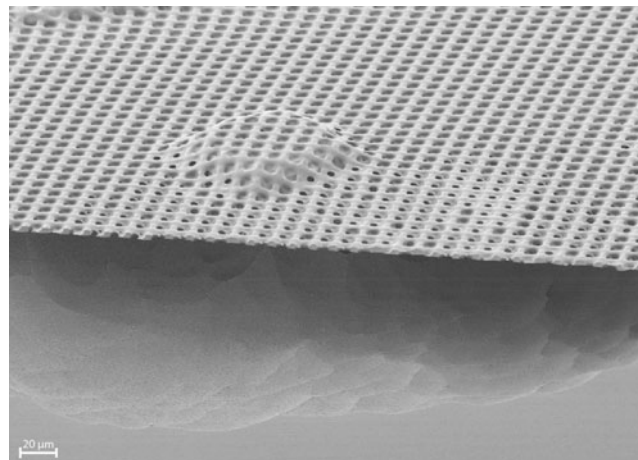


Fig. 6 Scanning electron microscopy image (cross sectional view achieved by cleaving the substrate) of a porous SU-8 membrane that was shaped over KOH-etched silicon pillars. Removal of the pillars was achieved with xenon difluoride gas that accessed the silicon through the membrane's pores. Etching the silicon underneath the membrane creates a microfluidic chamber. The membrane retained its three-dimensional character after silicon etching as well as after subsequent immersion in water, which is a necessary step for successful three-dimensional Caco-2 cell culture on it

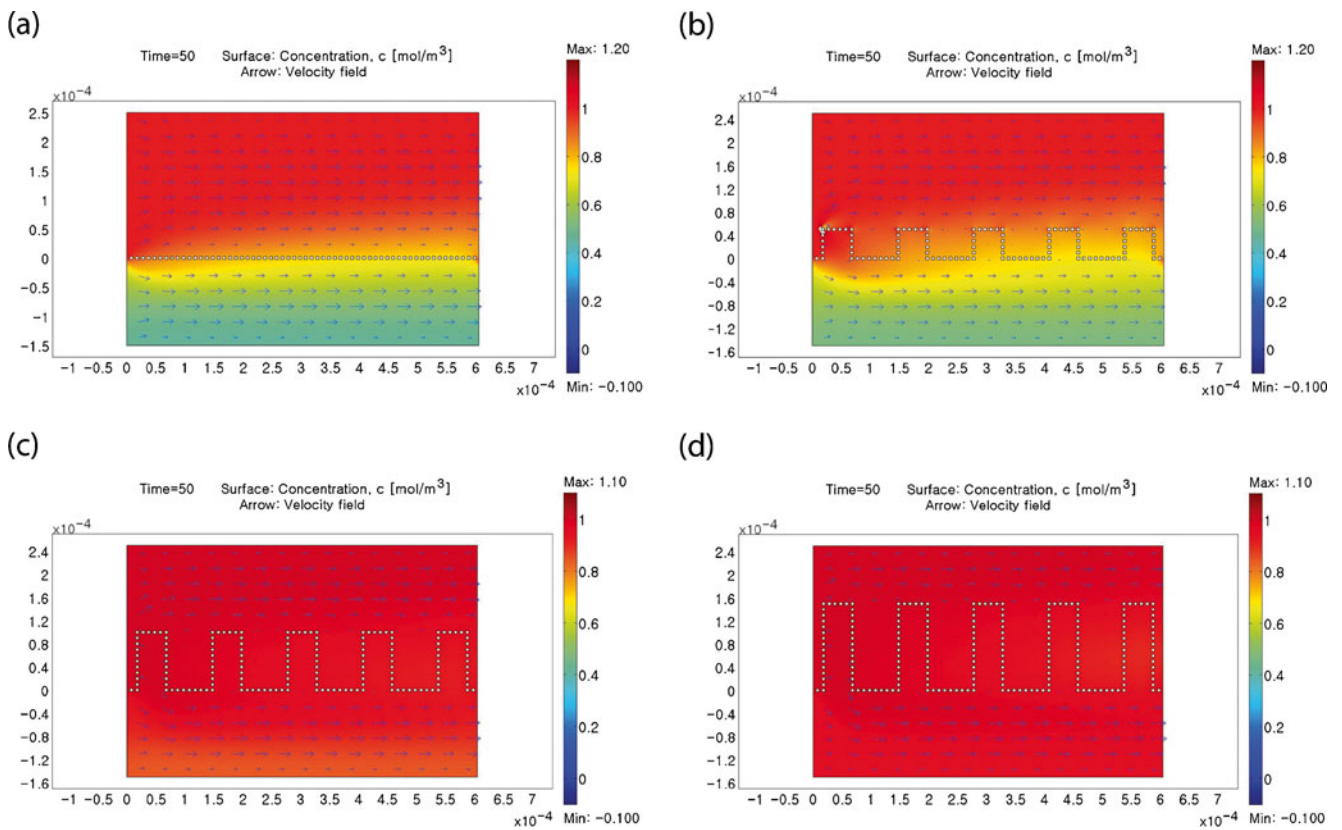


Fig. 7 Velocity (arrow) and concentration (color) profile after 50 s in the microfluidic device with SU-8 membrane. (a) A flat membrane (b) Membrane with aspect ratio of 1 (c) Membrane with aspect ratio of 2 (d) Membrane with aspect ratio of 3

Further, Caco-2 cells developed tight junctions on both types of membranes, indicating that the cell density has reached the critical level that is necessary to establish the barrier function of the model. Occludin is a protein that is part of tight junction complexes, which develop between all gastrointestinal epithelial cells when they come in close contact with each other. These junctions limit the transport of substances through the intercellular space (Furuse et al. 1993). They are a key feature of the *in vivo* epithelium of the gastrointestinal tract. Figure 3 (a) shows a fluorescence microscopy image of Caco-2 cells grown for 21 days on flat SU-8 membranes. The cells were fixed and immunostained for occludin. Visual inspection revealed that the membrane was fully covered with occludin-expressing Caco-2 cells.

On three-dimensional membrane surfaces, cells settled at the membrane’s valleys first and then spread onto the pillars. Figures 4 and 5 show confocal fluorescence images of the Caco-2 cells cultured on three-dimensional SU-8 membranes. Immunostaining for the nucleus (blue), actin (green), and occludin (red) after 8 days of culture and subsequent fluorescent imaging revealed that Caco-2 cells covered an estimated 80 % of the area at this time. The sidewalls of 50 μm high pillars were also covered, but not their top surfaces (Fig. 4(a, b, and c)). Occludin expression

was visible on many cells, but not visible throughout the entire cell layer, indicating that the cell density was yet too low for establishing the barrier function of the cell layer. After 21 days of cell culture the entire membrane area, including the side-walls and top surfaces of the pillars was covered with Caco-2 cells (100 % according to visual inspection) (Fig. 4(d, e, f)). Tight junctions as shown via occludin immunostaining were well developed throughout the cell layer (Fig. 4(e)).

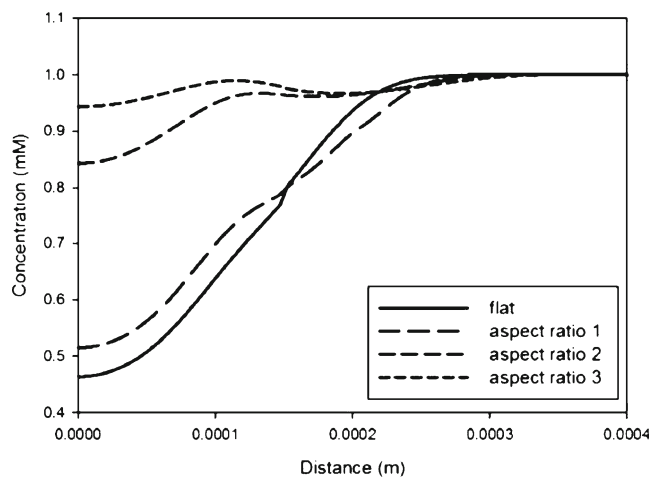


Fig. 8 Concentration profile across the top and bottom layers

When the spacing between the pillars was less than 100 μm , cells often merged into a single cell mass rather than forming separate pillar shapes. This phenomenon was more evident when cells were cultured for longer than 14 days. Within the combinations we tested, 50 or 100 μm wide pillars with 100 or 200 μm spacing gave the best coverage. This result is promising since the density of the pillar structures is close to that of human intestinal villi, which is about 25 villi per mm^2 (Tortora and Grabowski 1993). We are currently working on improving the fabrication method to achieve higher aspect ratio structures to mimic the human intestinal villi more accurately. *In vivo* the macro villi of the intestinal epithelium are approximately 500 μm high (Tortora and Grabowski 1993).

Since Caco-2 cells grew on all fabricated membranes with comparable morphology to that observed on commercially available membranes, we conclude that the fabricated membranes fulfill the requirements needed to culture epithelial cells on them. The requirements for this are that the membrane can span across microfluidic chambers that are several millimeters wide and long, that it is mechanically stable enough to support cell growth, and that it accommodates mass transport through the cell layer via pores. The pores must be large enough to enable the exchange of metabolites, but small enough to prevent cells from migrating through. At the same time, the membranes must be thin enough to allow for efficient transport of molecules and at the same time thick enough to withstand physical forces originating from cellular attachment and microfluidic flow. The membrane's mechanical stability was sufficient to support the culture of Caco-2 cells that formed tight junctions. The Caco-2 cells cultured on the fabricated membranes are an on chip *in vitro* model of the epithelium of the gastrointestinal tract that can be integrated with other organ compartments to create multi-organ cell culture devices for drug testing.

3.4 Creating varying chamber depths in microfluidic devices with flat and with three-dimensional porous membranes

The novelty of the proposed fabrication methods lies in the three-dimensional character of the membranes and in the ease with which they can be integrated with “body-on-a-chip” devices. To simulate the digestive system and the systemic circulation, two microfluidic streams that access the apical and basolateral sides of the Caco-2 cell layer separately from one another are needed. When fabricating flat membranes, the basolateral microfluidic chamber is created during the first exposure. This is immediately followed by a second exposure that creates the membrane. Only one development step is needed to yield a membrane that is attached to the chamber walls. The design is leak-free and the membrane does not need to be handled outside the fluidic device. No gaskets are needed to prevent leakage. Although it is possible to construct the apical chamber with SU-8 as well, we micromachined it into a plexiglass top piece that also contained an embedded electrode. The design lends itself to the integration of electrodes that can evaluate the quality of the barrier function of the epithelial cell layer.

Fluidic access to the basolateral chamber of systems with three-dimensionally shaped membranes is limited when the gap between the membrane and the chamber floor is created by dissolving a thin sacrificial layer that was spun on the wafer before SU-8 processing. To obtain better access to the basolateral side of the cells (i.e. the underside of the membrane), we dry etched the microfluidic chambers with xenon difluoride. Xenon difluoride diffused through the membrane's pores, accessed the silicon underneath and etched it isotropically. Using xenon difluoride at 4 Torr for 40 etch cycles that lasted 20 s each, we removed the silicon pillars and created a larger chamber depth (Fig. 6). Three-dimensionally shaped membranes retained their

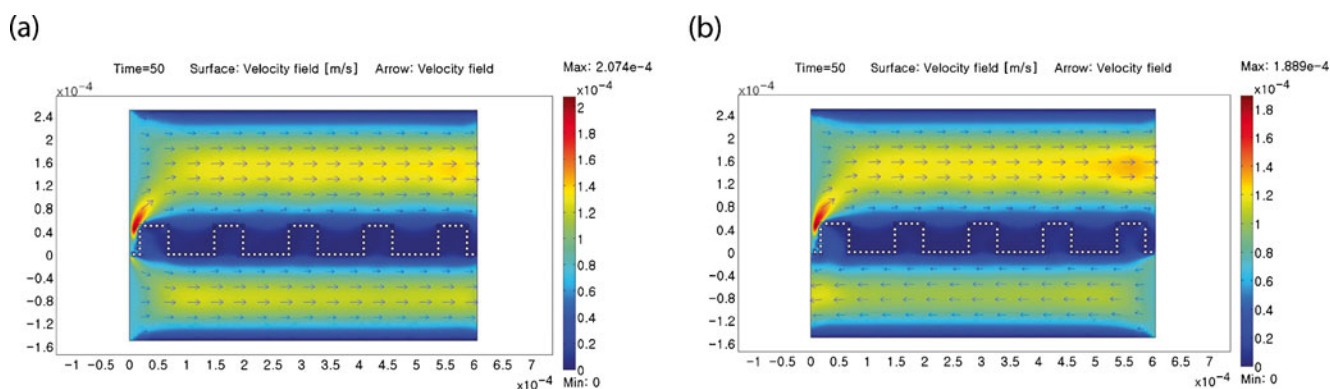


Fig. 9 Fluid velocity profiles in top and bottom layers (a) co-current (flows in the same direction) (b) counter-current (flows in opposite directions)

shape after etching as well as after immersion in water. Since *in vivo* villi structures have a much higher aspect ratio than the shapes presented here, we will need to further develop the fabrication protocol to achieve higher aspect ratio structures. However, the experiments discussed here present the first microfabricated porous membranes that are integral parts of microfluidic systems and that are shaped three-dimensionally.

Membranes with three-dimensional villi structures can be used to investigate hypotheses that aim to explain the difference in predictive value of mass transport across Caco-2 monolayers between fast and slowly absorbed drugs. While the absorption rate of fast absorbing drugs compares well to that seen *in vivo* (the absorption difference is only 2- to 4-fold) the absorption of slowly absorbed drugs is about 50-fold slower in the *in vitro* model compared to *in vivo*. This effect could be related to the smaller surface area that is available in the *in vitro* model due to the lack of macro villi (Artursson et al. 2001; Lennernas 1997). It has been theorized that drugs that slowly absorb concentrate at the villous tips, resulting in a concentration gradient that supports the drug's diffusion into the intervillous space (Schwartz et al. 1995). These hypotheses could be tested with microfluidic systems that were fabricated with the described methods.

3.5 Simulation of convection/diffusion profiles inside microfluidic chambers with three-dimensionally shaped membranes

Figure 7 shows the velocity (blue arrows) and concentration (color map) profiles after 50 s. Due to the obstruction of the pillars, the space between the pillars maintain almost stagnant flow pattern. As the height of the pillars increases, the area of stagnant flow becomes greater. Also the simulation result indicates that diffusion occurs quicker with increasing aspect ratio of the pillars. This can be explained by the increase in the permeable surface area with increasing aspect ratio. In addition, increasing the aspect ratio affects the flow velocity in the upper channel, increasing the velocity. A higher flow velocity results in a faster transport across the membrane. Figure 8 shows the plot of the concentration profiles across the height of the microfluidic device at time 50 s. When the aspect ratio is greater than 2, the concentration profile becomes much flatter. The convective mixing between the top and bottom layer was almost negligible, as the fabricated membrane with 5 μm pore size provides sufficient fluidic resistance. This was true regardless of the direction of the flows in the top and bottom layers (Fig. 9). Having opposite flow directions in the top and bottom

layers did not affect the diffusion profiles across the membranes, regardless of the aspect ratios of the pillars.

4 Summary

We report here the use of partial SU-8 cross-linking to create flat, porous membranes and porous membranes draped over three-dimensional silicon shapes. Caco-2 cells cultured on both types of membranes developed confluent layers with tight junctions. On membranes with 3-D shapes the cells conformed to the shape of the membrane during proliferation, forming villi-like shapes that are similar to those observed in the intestinal epithelium. Pores in the membranes (between 0.5–4 μm) enable mass transfer that is needed for drug absorption studies. The overall porosity was between 4.4 %–25.3 % and can be further increased by reducing the size of supporting posts underneath. To gain better access to the backside of three-dimensionally shaped membranes, we removed the underlying silicon via xenon difluoride etching. Our fabrication method is useful for creating better *in vitro* models of human barrier tissues, which can be used for drug screening.

Acknowledgments Financial support for this work was provided by the Nanobiotechnology Center (NBTC), an STC Program of the National Science Foundation, under Agreement No. ECS-9876771, by the Army Corps of Engineers under Agreement ID W9132T-07-2-0010 and by the NSF under grant No. CBET-1106153. This work was performed in part at the Cornell NanoScale Science & Technology Facility, a member of the National Nanotechnology Infrastructure Network, which is supported by the National Science Foundation (Grant ECS-0335765). This work was in part supported by the National Research Foundation of Korea (NRF, Grant no. 2012-0003408), KFRI (Korea Food Research Institute, grant no: E0121705), Hongik University new faculty research support fund, and 2012 Hongik University Research Fund. Caco-2 samples for SEM imaging were prepared at the Cornell Center for Materials Research (CCMR, NSF DMR-1120296).

References

- J.R. Anderson, D.T. Chiu, R.J. Jackman, O. Cherniavskaya, J.C. McDonald, H. Wu, S.H. Whitesides, G.M. Whitesides, *Anal. Chem.* **72**, 3158 (2000)
- P. Artursson, K. Palm, K. Luthman, *Adv. Drug Deliv. Rev.* **46**, 27 (2001)
- B. Bohl, R. Steger, R. Zengerle, P. Koltay, *J. Micromech. Microeng.* **15**, 1125 (2005)
- R.M. Brand, T.L. Hannah, C. Mueller, Y. Cetin, F.G. Hamel, *Ann. Biomed. Eng.* **28**, 1210 (2000)
- J. Carlier, S. Arscott, V. Thomy, J.C. Fourrier, F. Caron, J.C. Camart, C. Druon, P. Tabourier, *J. Micromech. Microeng.* **14**, 619 (2004)
- R.A. Conradi, K.F. Wilkinson, B.D. Rush, A.R. Hilgers, M.J. Ruwart, P.S. Burton, *Pharm. Res.* **10**, 1790 (1993)
- N. Ferrell, R.R. Desai, A.J. Fleischman, S. Roy, H.D. Humes, W.H. Fissell, *Biotechnol. Bioeng.* **107**, 707 (2010)
- M. Furuse, T. Hirase, M. Itoh, A. Nagafuchi, S. Yonemura, S. Tsukita, S. Tsukita, *J. Cell Biol.* **123**, 1777 (1993)

- G. Harris, M. Shuler, *Biotech. Bioproc. Eng.* **8**, 246 (2003)
- I. Hubatsch, E.G. Ragnarsson, P. Artursson, *Nat. Protoc.* **2**, 2111 (2007)
- D. Huh, B.D. Matthews, A. Mammoto, M. Montoya-Zavala, H.Y. Hsin, D.E. Ingber, *Science* **328**, 1662 (2010)
- Y. Imura, Y. Asano, K. Sato, E. Yoshimura, *Anal. Sci.* **25**, 1403 (2009)
- D.C. Kim, P.S. Burton, R.T. Borchardt, *Pharm. Res.* **10**, 1710 (1993)
- K. Kim, D.S. Park, H.M. Lu, W. Che, K. Kim, J. Lee, C.H. Ahn, *J. Micromech. Microeng.* **14**, 597 (2004)
- I. Kola, J. Landis, *Nat. Rev. Drug Discov.* **3**, 711 (2004)
- H. Lennernas, *J. Pharm. Pharmacol.* **49**, 627 (1997)
- B. Ma, G. Zhang, J. Qin, B. Lin, *B. Lin.* **9**, 232 (2009)
- G.J. Mahler, M.B. Esch, R.P. Glahn, M.L. Shuler, *Biotechnol. Bioeng.* **104**, 193 (2009a)
- G.J. Mahler, M.L. Shuler, R.P. Glahn, *J. Nutr. Biochem.* **20**, 494 (2009b)
- C. Ramello, P. Paullier, A. Ould-Dris, M. Monge, C. Legallais, E. Leclerc, *Toxicol. In Vitro* **25**, 1123 (2011)
- W. Rubas, M.E. Cromwell, Z. Shahrokh, J. Villagran, T.N. Nguyen, M. Wellton, T.H. Nguyen, R.J. Mrsny, *J. Pharm. Sci.* **85**, 165 (1996)
- R.M. Schwartz, J.K. Furne, M.D. Levitt, *Gastroenterology* **109**, 1206 (1995)
- A. Sin, K.C. Chin, M.F. Jamil, Y. Kostov, G. Rao, M.L. Shuler **20**, 338 (2004)
- J.H. Sung, J. Yu, D. Luo, M.L. Shuler, J.C. March, *Lab Chip* **11**, 389 (2011)
- D.A. Tatosian, M.L. Shuler **103**, 187 (2009)
- G.J. Tortora, S.R. Grabowski, *Principles of Anatomy and Physiology* (HarperCollinsCollege, New York, 1993)
- F. Vozzi, J.M. Heinrich, A. Bader, A.D. Ahluwalia **15**, 1291 (2009)
- L. Wang, S.K. Murthy, G.A. Barabino, R.L. Carrier, *Biomaterials* **31**, 7586 (2010)
- P. Wils, A. Warnery, V. Phung-Ba, D. Scherman, *Cell Biol. Toxicol.* **10**, 393 (1994)
- W.M. Zhang, J. Li, L.X. Cao, Y.G. Wang, W. Guo, K.X. Liu, J.M. Xue, *Nucl. Instrum. Meth. B* **266**, 3166 (2008)
- C. Zhang, Z. Zhao, N.A. Abdul Rahim, D. van Noort, H. Yu, *Lab Chip* **9**, 3185 (2009)